

Synthesis and properties of bay unilaterally extended and mono-substituted perylene diimides

Fengxia Zhang¹, Xianqiang Huang², Xiaofeng Wei¹, Huixue Ren¹,
Tianyi Jiang¹, Xuemei Li¹, Junsen Wu¹ and Yongshan Ma¹ 

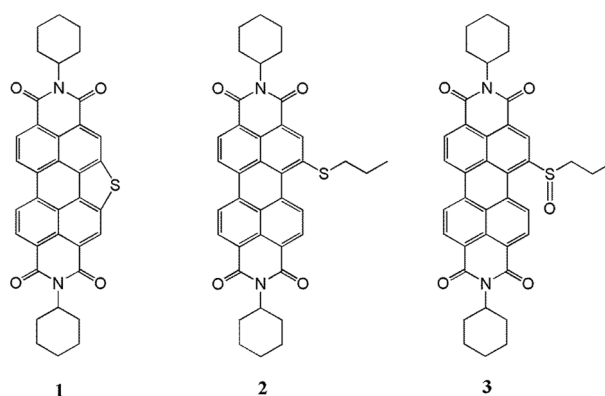
Abstract

The synthesis of two sulfur-decorated perylene diimides, the five-membered S-heterocyclic annulated perylene diimide (**1**) and 1-propanethiol-*N,N'*-dicyclohexylperylene-3,4,9,10-tetracarboxylic diimide (**2**), and a novel sulfoxide-containing perylene diimide, 1-propyl sulfoxide-*N,N'*-dicyclohexylperylene-3,4,9,10-tetracarboxylic diimide (**3**), are reported. The photophysical, electrochemical, aggregation, and thermal properties of these compounds are investigated by ultraviolet visible absorption, fluorescence, cyclic voltammetric, X-ray diffraction, and thermogravimetric analysis techniques. The geometries of the compounds are optimized at the 6-31G* level of theory using density functional theory, and their potentials are correlated with molecular orbitals. The prepared perylene diimide derivatives exhibit narrow the highest occupied molecular orbitals and the lowest unoccupied molecular orbitals band gaps, and they have quite different absorptions and emissions in dichloromethane solutions, which are in agreement with the density functional theory-calculated results.

Keywords

absorption, density functional theory, electrochemical, fluorescence, perylene diimide, X-ray diffraction

Date received: 9 April 2019; accepted: 14 October 2019



¹School of Municipal and Environmental Engineering, Shandong Jianzhu University, Jinan, P.R. China

²Shandong Provincial Key Laboratory of Chemical Energy Storage and Novel Cell Technology, College of Chemistry and Chemical Engineering, Liaocheng University, Liaocheng, P.R. China

Corresponding authors:

Junsen Wu, School of Municipal and Environmental Engineering, Shandong Jianzhu University, Jinan 250101, P.R. China.
Email: wujunsen@sdjzu.edu.cn

Yongshan Ma, School of Municipal and Environmental Engineering, Shandong Jianzhu University, Jinan 250101, P.R. China.
Email: mlosh@sdjzu.edu.cn

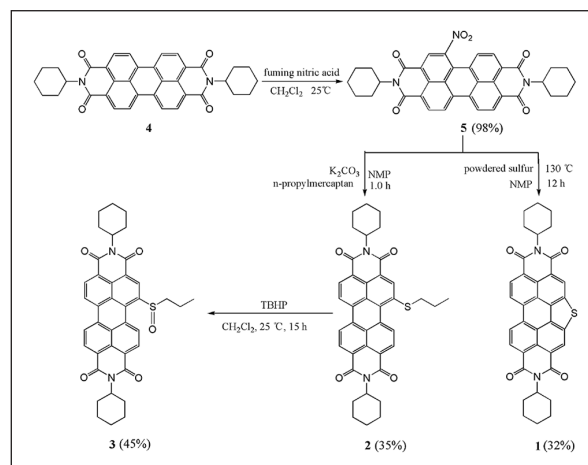
Introduction

Polycyclic aromatic hydrocarbons (PAHs) have attracted considerable interest from researchers in different fields due to their unique optical and electrochemical properties.^{1–3} The synthesis, properties, and applications of PAHs have become a rapidly developing scientific field.⁴ As a category of PAHs, perylene diimides (PDIs) have high fluorescence quantum yields and excellent photochemical and thermal stabilities.⁵ Moreover, they are versatile candidates for applications in organic photovoltaics (OPVs), organic field-effect transistors (OFETs), and organic light-emitting diodes (OLEDs).^{6–9} Thus, establishing efficient routes for the synthesis of PDIs is very important. Most modification strategies can be classified into two categories. The first involves incorporating functional groups on the aromatic backbone of the imide, ortho, or bay positions of the PDIs.^{10–12} The second is extending the π -systems by the incorporation of heteroatoms (such as B, N, S, Se, O, and Si) into the frameworks of the aromatic rings.¹³ Modifying the imide substituents has a vital effects on the electronic structures and properties of PDIs because the imide nitrogen atoms are the nodal points of frontier orbitals.^{14,15} Attaching various substitutions at the bay position of PDIs should be another promising strategy for modifying the frontier orbital levels.¹⁶

Fully fused bay-modification of PDIs has been demonstrated to enhance their electronic and optoelectronic properties.^{17,18} Extensions along the short molecular axis of PDIs cause a hypsochromic shift of absorption spectra and induce a variety of intermolecular interactions. These interactions are essential to achieve highly ordered supramolecular self-assembled structures, which result in excellent device performance.^{19,20} Introducing heteroatoms to a π -conjugated system is also an easy approach for the construction of intramolecular charge-transfer compounds because the lone pairs of electrons of heteroatoms can be used as electron donors.²¹

An alkyl side chain is often selected as a soluble group. Its flexibility and small steric hindrance lead to minor effects on intermolecular approach but cause strong π - π stacking of adjacent perylene molecules. Sometimes, alkyl groups even facilitate the formation of ordered structures of perylene molecules through interdigitated actions.²² Due to the planar molecular geometry, PDIs with flexible linear alkyl substituents usually have high charge carrier mobility but low solid-state luminescence efficiency, which is a prerequisite for efficient optoelectronic and organic electronic devices.²³ As important structural motifs, sulfoxides have attracted increasing attention in recent years due to their unique properties such as central chirality at the sulfur, strong polarized S–O bond, and high configurational stability. In addition, organic sulfoxides have also been successfully used as steering ligands in transition-metal catalysis, new pharmacophores in drug discovery, and as versatile synthetic intermediates in the generation of natural and biologically active compounds.^{24,25}

In our previous work, two bay unilaterally extended PDIs, a five-membered O-heterocyclic annulated perylene diimide (O-PDI), and five-membered S-heterocyclic annulated PDI



Scheme 1. Synthesis of compounds **1–3**.

(**1**) have been synthesized (Scheme 1).²⁰ Comparing with O-PDI, the solubility of **1** improved and the absorbance maximum exhibited a hypsochromic shift. These properties made us interested in further exploring sulfur-decorated PDIs. In this work, we report the investigation of the unilaterally extended perylene derivative (compound **1**) and two mono-substituted perylene derivatives: 1-propylthio-*N,N'*-dicyclohexylperylene-3,4,9,10-tetracarboxylic diimide (**2**) and 1-propylsulfoxide-*N,N'*-dicyclohexylperylene-3,4,9,10-tetracarboxylic diimide (**3**). This is the first report of unsymmetrical sulfoxide-decorated PDI derivatives. Due to their different configurations and electron-donating abilities, the three compounds exhibited different photophysical, electrochemical, and aggregation properties.

Results and discussion

Synthesis and characterization

Scheme 1 shows the chemical structures and synthetic routes toward bay unilaterally extended **1** and mono-substituted **2** and **3** PDIs. The synthesis started with the imidization of PDI by reaction with cyclohexylamine. Compound **5** can then be achieved by the reaction of compound **4** with cerium(IV) ammonium nitrate [$\text{Ce}(\text{NH}_4)_2(\text{NO}_3)_6$] and nitric acid at ambient temperature. Substitution of the nitro group of **5** with an S atom group and a propylthio group were performed to obtain the corresponding products **1** and **2**. The transfer of an oxygen atom to a sulfide substrate can be achieved by treatment of compound **2** with *tert*-butyl hydroperoxide (TBHP) in dichloromethane at 25°C for 15 h. **CAUTION:** TBHP is dangerous and it should be used by experienced practitioners of organic synthesis using appropriate safety equipment. TBHP can be stored under nitrogen in a freezer at -20°C for prolonged periods of time (from months up to a year) without degradation or loss of reactivity. The structures of the three sulfur-decorated PDIs (**1–3**) have been fully characterized through nuclear magnetic resonance (NMR) (^1H NMR for compounds **1** and **3**, ^1H and ^{13}C NMR for compound **2**), Fourier-transform infrared (FTIR), and high-resolution mass spectrometry (HRMS) (see the Supplemental material). Because of the

poor solubilities of compounds **1** and **3**, we were unable to observe their ^{13}C NMR spectra. In the ^1H NMR spectrum of compound **2**, three characteristic signals (8.57, 8.46, and 8.23 ppm) were observed at low field. The corresponding signals were observed at 9.85, 8.66, and 8.46 ppm for compound **3**, which had shifted to relatively lower field due to the introduction of the electron-withdrawing sulfoxide group.

Optical properties

The optical properties of compounds **1–5** in dichloromethane at room temperature were investigated by ultraviolet visible (UV-Vis) absorption (Figure 1) and fluorescence spectroscopy (Figure 2). The spectra of compound **1** showed two well-defined vibronic $\pi-\pi^*$ transition absorption bands (497 and 467 nm) and a broad shoulder peak around 439 nm. The spectra were in accord with the characteristics of the 0–0, 0–1, and 0–2 transition energy. The absorption peaks of compound **4** appeared at 525 and 488 nm with a shoulder around 457 nm, and are blue shifted for **1** compared with its parent compound **4** as a reflection of the extended aromatic core along the short molecular axis.¹⁷ The UV-Vis absorption spectrum of **5** is nearly identical with the spectrum of the non-substituted perylene bisimide (**4**), but it did not exhibit fluorescence. In comparison with compound **4**, the maximum absorption of **2** is bathochromically shifted by about 12 nm. Notably, introduction of the electron-donating propylthio group induces a red shift, and therefore, **2** exhibited significant differences in absorptive features compared with compounds **1** and **4**. On the contrary, the oxidation of **2** to **3** switches the substituent from an electron-donating group to an electron-withdrawing group and causes a blue shift. Due to the charge-transfer absorption, the spectra of **2** and **3** are dominated by broad absorption bands that span a large part of the visible spectrum (400–650 nm).²⁶ Moreover, the longest wavelength absorption band of **1–3** exhibits a red shift when the solvent polarity was increased (Table 1).

The fluorescence spectra depicted the same structure with a mirror image of the absorption spectra, and the emission peaks appeared at 511 and 542 nm for compounds **1** and **4**, respectively. The maximum emission band of **2** shifted significantly to the red and is located at 611 nm, and is blue shifted to 554 nm for **3**. The PDIs presented

here possess Stokes shifts of about 14, 74, and 21 nm for **1–3**, respectively. The fluorescence spectra of compounds **1–3** were red shifted with the increase of solvent polarity (Figure 3), indicating strong intramolecular charge transfer (ICT) characteristics for the excited states of **1–3**.

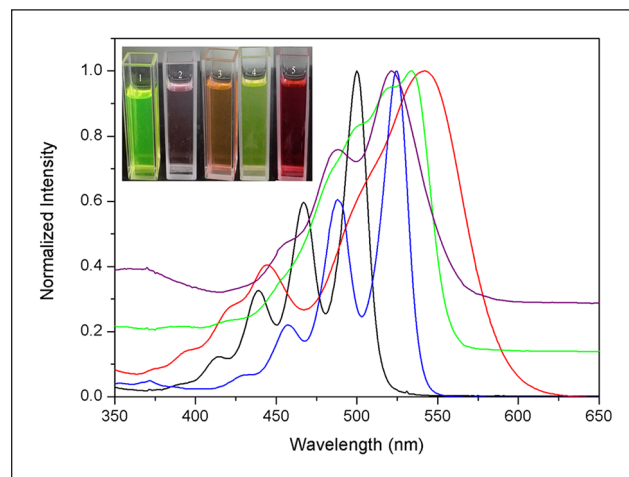


Figure 1. Normalized absorption spectra of **1** (black line), **2** (red line), **3** (green line), **4** (blue line), and **5** (purple line) in dichloromethane recorded at room temperature.

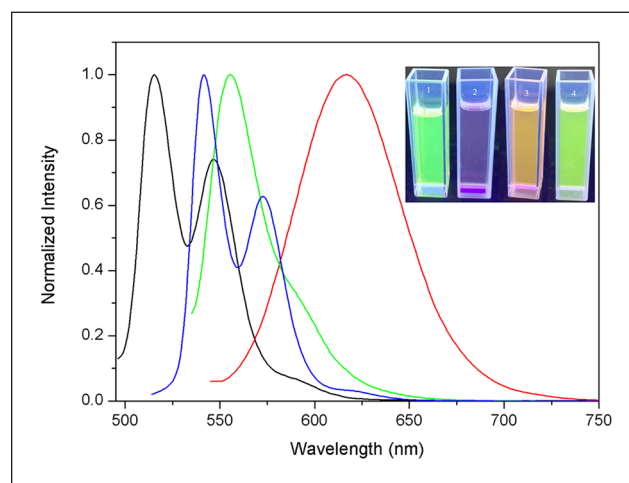


Figure 2. Normalized fluorescence spectra of **1** (black line), **2** (red line), **3** (green line), and **4** (blue line) in dichloromethane recorded at room temperature.

Table 1. Summary of the optical absorption and emission properties of **1–3** in various solvents.

Compound ^a		Cyclohexane	Ethyl acetate	Dichloromethane	Tetrahydrofuran
1 ^b	λ_{abs} (nm)	494	495	497	500
	λ_{em} (nm)	500	508	511	515
2 ^c	λ_{abs} (nm)	534	535	537	542
	λ_{em} (nm)	590	610	611	616
3 ^d	λ_{abs} (nm)	529	528	532	533
	λ_{em} (nm)	550	552	553	557

^aMeasured at 10^{-5} M.

^b $\lambda_{\text{ex}} \approx 497$ nm.

^c $\lambda_{\text{ex}} \approx 537$ nm.

^d $\lambda_{\text{ex}} \approx 532$ nm.

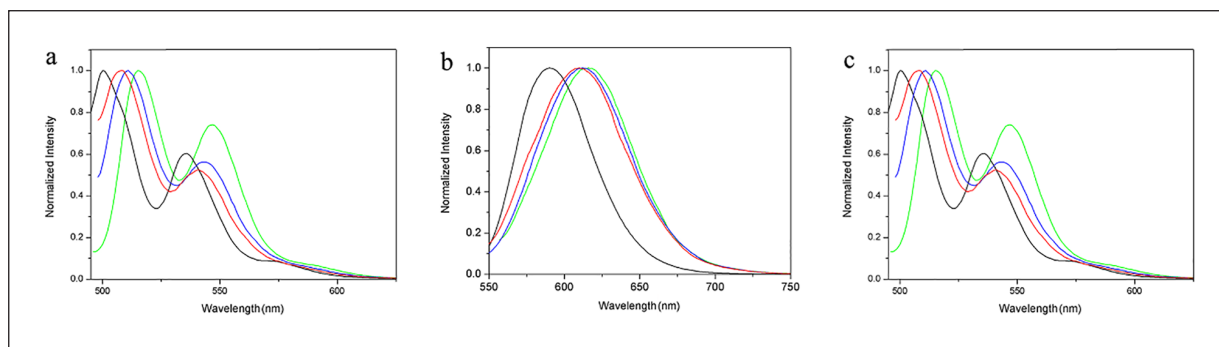


Figure 3. Normalized emission spectra of **1** (a), **2** (b), and **3** (c) in cyclohexane (black line), ethyl acetate (red line), tetrahydrofuran (green line), and dichloromethane (blue line).

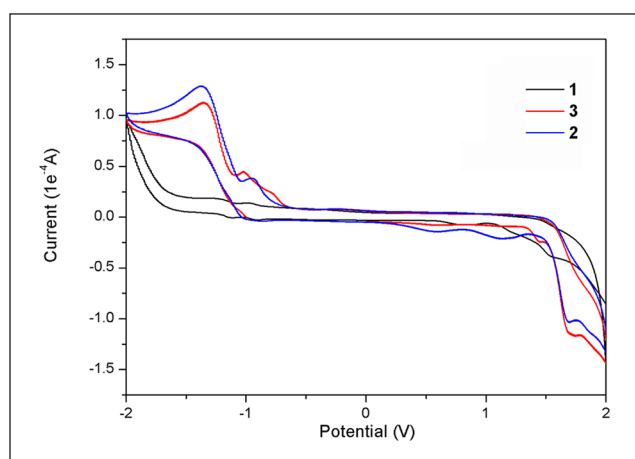


Figure 4. The cyclic voltammograms of **1–3** in CH_2Cl_2 (under N_2 atmosphere, scanning rate 20 mV/s) using Bu_4NPF_6 as the electrolyte, a glassy carbon electrode as the working electrode, platinum as the counter electrode, and Ag/AgNO_3 as the reference electrode.

Electrochemical properties

The cyclic voltammograms of **1–3** are illustrated in Figure 4, and their redox potentials and energy levels are summarized in Table 2. These chromophores undergo reversible reduction and oxidation waves. Compounds **1** and **3** showed two reduction peaks, implying their ability to accept at least two electrons. The HOMO-LUMO (the highest occupied molecular orbitals and the lowest unoccupied molecular orbitals) energy levels of **1–3** are estimated to be $-6.35/-3.80$, $-5.94/-3.85$, and $-6.25/-4.02$ eV, respectively. As expected, the trend of the HOMO-LUMO energy gap is **1** > **3** > **2**, which is in agreement with the optical band gap energies (E_g^b) (Table 3) derived from the onset absorption edges in solutions.

Quantum chemistry computations

To gain insight into the electronic properties of **1–3**, quantum chemical calculations were carried out with density functional theory (DFT) at the B3LYP/6-31G* level. Figure 5 shows the HOMOs and LUMOs of **1–3**. It can be noted that the HOMO of **1** is centered on the perylene ring system and that the LUMO is extended from the central perylene core to

the heteroatom and the bisimide groups. The HOMO of **2** is delocalized on the perylene core and S heteroatom sites, while the LUMO is centered on the perylene ring system. The HOMO of **3** is centered on the sulfoxide site, while the LUMO is delocalized on the perylene ring system. Compared with **4**, the band gap of **2** and **3** decreased due to the introduction of the alkyl sulfide and sulfoxide onto the perylene core, while the band gap of compound **1** increased due to the annulation as an S-heterocycle (Table 3). The optimized ground-state geometric conformations of **1–3** are shown in Figure 6. All atoms of the perylene skeleton and the S of S-heterocyclic annulated perylene diimide (compound **1**) are of planar conformation. However, the ground-state geometries of the perylene core of compounds **2** and **3** have two core twist angles. The dihedral angles between the two naphthalene subunits attached onto the central benzene ring were calculated to be about 4.65° and 3.32° for **2**, and 4.97° and 4.13° for **3**. Thus, the introduction of an alkyl sulfide and sulfoxide into the perylene skeleton broke down the original planar conformation of the perylene and enlarged the dihedral angles slightly. The entire backbone of **1** possessed a highly planar geometry, which correlated well with the reported crystal structure confirmed by X-ray crystallographic analysis.²⁰

Powder X-ray diffraction studies

The structures of PDIs **1–3** in the powder state were investigated by X-ray diffraction (XRD) experiments. As shown in Figure 7, the XRD data of **1** displays a greater number of diffraction peaks between 5° and 50° with a clear diffraction peak at $2\theta=5.05^\circ$ (1.73 nm), which is in accord with the diffraction from the (001) planes of the α -form crystal.²⁷ The peak at 24.35° corresponding to a distance of 0.36 nm can be attributed to the π - π stacking distance of PDI rings between the adjacent molecules. In contrast to **1**, the XRD pattern of **2** shows two clear diffraction peaks at $2\theta=5.62^\circ$ (1.56 nm) and $2\theta=8.44^\circ$ (1.05 nm), which correspond to the diffractions from the (100) and (010) planes, respectively. In addition, the diffraction peak at 25.6° (0.34 nm) can be attributed to the π - π stacking of the adjacent PDI. The XRD diagram of **3** shows a wide diffraction peak at 22.8° (0.38 nm). The wider diffraction peaks in **3** indicate that its degree of molecular order in the solid state was lower than compared with **2**. The d value of the (001) planes and the distance between the adjacent molecules of **3** are comparable with those of **2**. This

Table 2. Electrochemical data of compounds **1–3**.

Molecule	E_{redI} (V) ^a	E_{LUMO} (eV) ^b	E_{oxI} (V) ^a	E_{HOMO} (eV) ^b	E_{gap} (eV) ^b
1	−0.999	−3.80	1.551	−6.35	2.55
2	−0.95	−3.85	1.14	−5.94	2.09
3	−0.78	−4.02	1.45	−6.25	2.23

^aMeasured in a solution of 0.1 M tetrabutylammonium hexafluorophosphate (TBAPF₆) in dichloromethane versus Ag/AgNO₃ (in Volts).

^bCalculated from $E_{\text{HOMO}} = -4.88 - (E_{\text{oxd}} - E_{\text{FeI/FeI}^+})$, $E_{\text{LUMO}} = E_{\text{HOMO}} + E_{\text{gap}}$.

Table 3. Calculated and experimental parameters for compounds **1–4**.

Compound	HOMO ^a	LUMO ^a	E_g^a	E_g^b	Twisting angle (°)
1	−6.26	−3.62	2.64	2.49	0
2	−5.99	−3.54	2.45	2.31	4.65, 3.32
3	−6.22	−3.73	2.49	2.33	4.97, 4.13
4	−6.19	−3.62	2.57	2.36	0

HOMO: highest occupied molecular orbital; LUMO: lowest unoccupied molecular orbital.

^aCalculated by density functional theory (DFT)/B3LYP (in eV).

^bAt absorption maxima ($E_g = 1240/\lambda_{\text{max}}$, in eV).

indicates that the solid-state structures of bay mono-substituted PDIs are related to the substituent group at the bay position of the perylene core. In the case of **3**, the sulfoxide substituent resulted in an increase of the distances of the (010) plane and π - π stacking. A diffraction peak at $2\theta = 15.7^\circ$ (d spacing 0.56 nm) was observed in the diffraction pattern of **1**, which is shifted to 16.86° (d spacing 0.53 nm) in the diffraction of **2** and 16.51° (d spacing 0.52 nm) in the diffraction of **3**. The shift can be attributed to the α -form crystals.

Finally, thermogravimetric analysis (TGA) of **1–3** was conducted under a nitrogen atmosphere, and the thermograms are shown in Figure 8. The decomposition temperatures (5% weight loss) were all higher than 350°C . Similar to other PDIs, compounds **1–3** in solution and solid state were very stable. The remarkable thermal and photooxidation stability were promising for use in organic semiconductor devices.

Conclusion

This study describes the synthesis of three sulfur-decorated PDIs equipped with different substituents and the impact of the structures on their photophysical, electrochemical, aggregation, and thermal properties. The HOMO, LUMO, and energy gaps obtained through DFT calculations are close to the experimental cyclic voltammetry (CV) values. These PDIs possess excellent photooxidative resistance, and demonstrate good solubility, as well as green and red colors in the neutral state derived from absorption in the visible region. Our study may be useful for the development of new PDIs that can be used as organic electronic materials.

Experimental

Materials and equipments

The solvents were purchased from commercial sources and used as received. *N,N'*-Dicyclohexyl-3,4,9,10-tetracarboxylic

acid bisimide (compound **4**) and *N,N'*-Dicyclohexyl-1-nitroperylene-3,4,9,10-tetracarboxylic acid bisimide (compound **5**) were synthesized according to the literature procedure.²⁸

The ¹H and ¹³C NMR spectra were obtained in CDCl₃ on a Bruker (Germany) 300 MHz spectrometer. FTIR spectra were measured on a Bruker Tensor-27 spectrophotometer. Mass spectra were measured on a Bruker MaXis UHR-TOF mass spectrometer. The absorption and emission spectra were recorded on a Varian (America) Cary 50 spectrophotometer and a Hitachi (Japan) FL-4500 spectrofluorometer. CV was performed with a CHI760E electrochemical analyzer at a potential rate of 100mV s^{-1} in a 0.1 M solution of tetrabutylammonium perchlorate (Bu₄NClO₄) in dichloromethane. Glassy carbon, platinum, and Ag/AgNO₃ electrodes were used as working, counter, and reference electrodes, respectively.

Computation details

Structure optimizations and property calculations employed Becke's three-parameter gradient-corrected hybrid density function B3LYP method and the standard 6-31G*(d) basis set.²⁹

Synthesis and characterization

Preparation of compound 1. Compound **1** was synthesized according to the literature procedure.²⁰ Compound **5** (180 mg, 0.3 mmol) and powdered sulfur (160 mg, 5.0 mmol) was dissolved in *N*-methylpyrrolidone (NMP), (10 mL). The resulting solution was stirred at 130°C under an argon atmosphere for 12 h and then poured into 2 M HCl (100 mL). The precipitate was collected and then washed with water. The crude product was purified by silica gel column chromatography with CH₂Cl₂/petroleum ether (5:2) as eluent to give PDI **1** as a bright yellow solid (36 mg, 32%). m.p.: $300\text{--}302^\circ\text{C}$. ¹H NMR (300 MHz, CHCl₃, TMS, ppm): δ 9.31 (s, 2H), 8.96 (d, 2H, $J = 8.1$ Hz), 8.90 (d, 2H, $J = 8.1$ Hz), 5.17 (m, 2H), 2.66 (m, 4H), 1.94 (m, 4H), 1.84 (m, 6H), 1.47–1.38 (m, 6H). FTIR (KBr, cm^{−1}): $\nu = 2917, 1698, 1648, 1593, 1426, 1349, 1303, 1234, 1175, 989, 889, 850, 803, 784, 735, 683, 628, 594, 449$. MS (APCI): m/z (relative intensity, %) 584 (100), 529 (2), 517 (4); HRMS (ionization technique): m/z [m]⁺ calcd. for C₃₆H₂₈N₂O₄S: 584.1800, found 584.1729. Elemental anal. calcd. (%) for C₃₆H₂₈N₂O₄S: C, 73.95; H, 4.83; N, 4.79; S, 5.48; found: C, 72.49; H, 4.67; N, 4.82; S, 5.87.

Preparation of compound 2. Compound **5** (1.0 g, 1.7 mmol) and K₂CO₃ (1.0 g) were suspended in NMP (50 mL) at

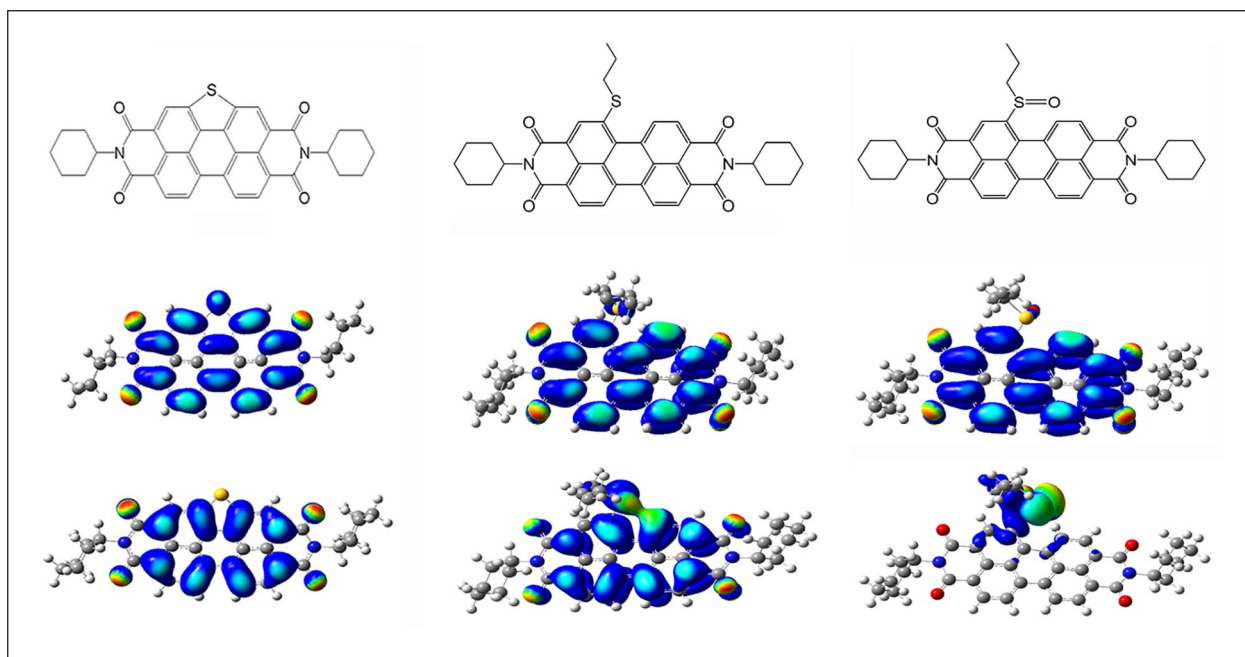


Figure 5. Computed frontier orbitals of **1–3**.
The upper plots are the LUMOs and the lower are the HOMOs.

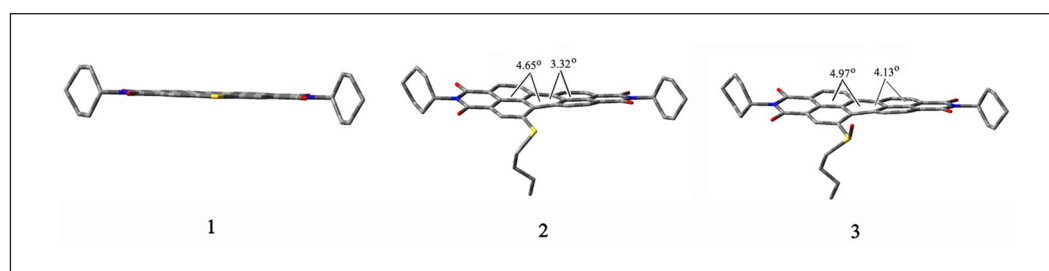


Figure 6. Optimized structures of **1–3** obtained by DFT calculations at the B3LYP/6-31G* level.
The gray, blue, red, and yellow balls represent C, N, O, and S atoms, respectively. The H atoms are omitted for clarity.

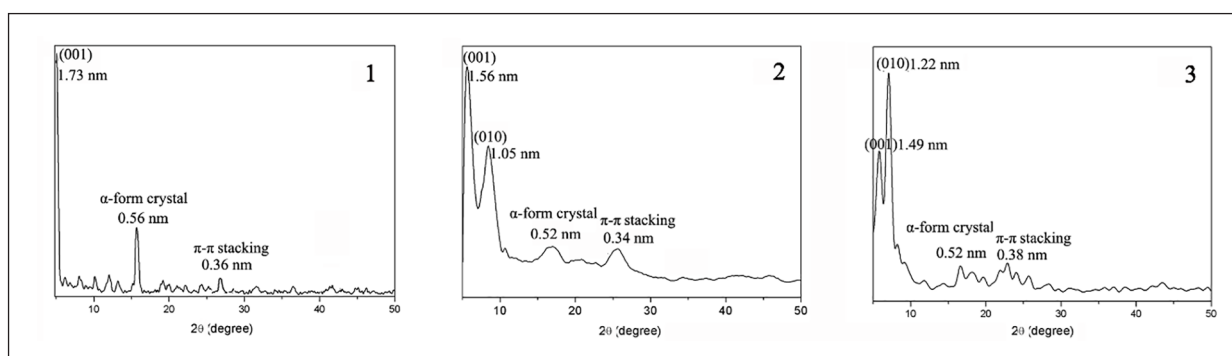


Figure 7. X-ray diffraction patterns of the PDIs **1–3**.

room temperature. *n*-Propyl mercaptan (20.0 mL, 2.2 mmol) was added to the solution, and the reaction mixture was stirred for 60 min at room temperature. It was then poured into 2 M HCl (300 mL). The precipitate was collected by vacuum filtration and washed with water three times (3×100 mL). The crude product was purified by silica gel column chromatography with CH_2Cl_2 /petroleum ether (4:1) as eluent to give PDI **2** as a red solid (375 mg, 35%).

m.p.: 297–299°C. ^1H NMR (300 MHz, CDCl_3 , TMS, ppm): δ 8.57 (m, 3H), 8.46–8.35 (m, 3H), 8.23 (s, 1H), 4.96 (m, 2H), 3.06 (m, 2H), 2.50 (m, 5H), 1.74 (m, 4H), 1.64 (m, 6H), 1.41 (m, 8H), 0.80–1.00 (m, 2H). ^{13}C NMR (75 MHz, CDCl_3 , ppm): δ 163.64, 139.58, 130.47, 129.24, 128.41, 127.27, 126.51, 125.96, 123.11, 122.72, 121.99, 54.18, 37.95, 29.13, 26.60, 25.49, 21.91, 13.61. FTIR (KBr, cm^{-1}): ν = 2922, 2845, 1691, 1651, 1611, 1415, 1343, 1307, 1257,

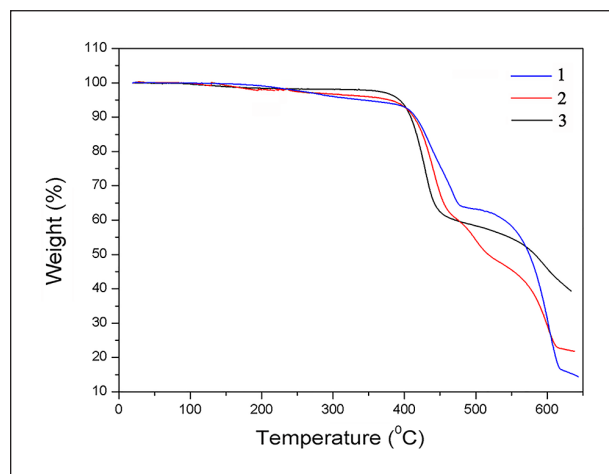


Figure 8. TGA curves of I–3.

1179, 1000, 894, 853, 804, 735, 629, 578, 448, 416. MS (APCI): m/z (relative intensity, %) 628 (100), 602 (1); HRMS (ionization technique): m/z [m]⁺ calcd. for C₃₉H₃₆N₂O₄S: 628.2401; found 628.2340. Elemental anal. calcd. (%) for C₃₉H₃₆N₂O₄S: C, 74.50; H, 5.77; N, 4.46; S, 5.10; found: C, 73.62; H, 4.98; N, 4.63; S, 5.21.

Preparation of compound 3. Compound 2 (200 mg, 0.32 mmol) was suspended in CH₂Cl₂ (20 mL) at room temperature. TBHP (0.8 mL, 70% solution in water, 0.5 mmol) was then added and the reaction mixture was stirred for 15 h at room temperature. After being cooled to room temperature, the solution was filtered and evaporated to dryness. The crude product was purified by silica gel column chromatography with CH₂Cl₂/petroleum ether (4:1) as the eluent to give PDI 3 as a red solid (95 mg, 45%). m.p.: 293–295°C. ¹H NMR (300 MHz, CDCl₃, TMS, ppm): δ 9.85 (m, 3H), 8.66–8.55 (m, 3H), 8.46 (s, 1H), 5.35 (m, 2H), 4.62 (m, 2H), 2.58 (m, 5H), 1.91 (m, 4H), 1.74 (m, 6H), 1.26 (m, 8H), 0.88 (m, 2H). FTIR (KBr, cm⁻¹): ν=2918, 2848, 1704, 1651, 1587, 1446, 1398, 1334, 1248, 1188, 1118, 1054, 979, 802, 742, 673, 448. MS (APCI): m/z (relative intensity, %) 644 (100); HRMS (ionization technique): m/z [m]⁺ calcd. for C₃₉H₃₆N₂O₅S: 644.2308; found 644.2300. Elemental anal. calcd. (%) for C₃₉H₃₆N₂O₅S: C, 72.65; H, 5.63; N, 4.34; S, 4.97; found: C, 71.82; H, 5.45; N, 4.63; S, 4.54.

Declaration of conflicting interests

The author(s) declared no potential conflicts of interest with respect to the research, authorship, and/or publication of this article.

Funding

The author(s) disclosed receipt of the following financial support for the research, authorship, and/or publication of this article: This work was supported by the Doctoral Foundation of Shandong Jianzhu University (grant nos. XNBS1938 and XNBS1712), the Science and Technology Plan Project of Housing and Urban-Rural

Construction Department in Shandong Province (grant nos. 2018-K11-01 and 2018-K7-01), the National Natural Science Foundation of China (grant no. 21871125), the Natural Science Foundation of Shandong Province (grant no. ZR2016EEM01), the National Key R&D Program of China (grant no. 2017YFF0209904), and the Science and Technology Project of MOHURD (grant no. 2015-K7-005).

ORCID iD

Yongshan Ma  <https://orcid.org/0000-0003-0652-5695>

Supplemental material

Supplemental material for this article is available online.

References

- Xiao K, Liu Y, Qi T, et al. *J Am Chem Soc* 2005; 127: 13281.
- Qian H, Liu C, Wang Z, et al. *Chem Commun* 2006; 44: 4587.
- Cormier RA and Gregg BA. *RSC Adv* 2014; 5: 2368.
- Sun Y, Tan L, Jiang S, et al. *J Am Chem Soc* 2007; 129: 1882.
- Jiang W, Qian HL, Li Y, et al. *J Org Chem* 2008; 73: 7369.
- Zhao GJ and Han KL. *J Phys Chem A* 2009; 113: 4788.
- Wei Q, Wang W, Zhou E, et al. *J Colloid Interf Sci* 2017; 504: 58.
- Würthner F, Saha-Möller CR, Fimmel B, et al. *Chem Rev* 2016; 116: 962.
- Chen S, Slattum P, Wang C, et al. *Chem Rev* 2015; 115: 11967.
- Görl D, Zhang X and Würthner F. *Angew Chem Int Ed* 2012; 51: 6328.
- Zang L, Che YK and Moore JS. *Acc Chem Res* 2008; 41: 1596.
- Zhao Q, Zhang S, Liu Y, et al. *J Mater Chem* 2012; 22: 7387.
- Zhu M, Zhuo Y, Guo H, et al. *J Lumin* 2018; 194: 264.
- Sun JP, Hendsbee AD, Dobson AJ, et al. *Org Electron* 2016; 35: 151.
- Nagarajan K, Mallia AR, Reddy VS, et al. *J Phys Chem C* 2016; 120: 8443.
- Mustafa EO, Samuel AS, Obaidullah M, et al. *J Lumin* 2017; 192: 414.
- Langhals H and Kirner S. *Eur J Org Chem* 2000; 28: 365.
- Li Y, Liu T, Liu H, et al. *Acc Chem Res* 2014; 47: 1186.
- Muth MA, Carrasco OM and Thelakkat M. *Adv Funct Mater* 2011; 21: 4510.
- Ma Y, Shi Z, Zhang A, et al. *Dyes Pigments* 2016; 135: 41.
- El-Mansy M and El-Nahass M. *Spectrochim Acta A* 2014; 130: 568.
- Echeverry CA, Cotta R, Insuasty A, et al. *Dyes Pigments* 2018; 153: 182.
- Zhang L and Cole JM. *J Mater Chem A* 2017; 5: 19541.
- Gan S, Yin J, Yao Y, et al. *Org Biomol Chem* 2017; 15: 2647.
- Ghosh S, Alghunaim AS, Al-Mashhadani MH, et al. *J Mater Chem C* 2018; 6: 3762.
- Chen KY and Chow TJ. *Tetrahedron Lett* 2010; 51: 5959.
- Ong KK, Jensen JO and Hameka HF. *J Mol Struct-THEOCHEM* 1999; 459: 131.
- Ahrens MJ, Tauber MJ and Wasielewski MR. *J Org Chem* 2006; 71: 2107.
- Miyata T and Masuko T. *Polymer* 1997; 38: 4003.